

## Study of $B \rightarrow \phi\phi K$ Decays

Y.-T. Shen,<sup>25</sup> K.-F. Chen,<sup>25</sup> P. Chang,<sup>25</sup> I. Adachi,<sup>7</sup> H. Aihara,<sup>40</sup> K. Arinstein,<sup>1</sup> T. Aushev,<sup>17,11</sup> A. M. Bakich,<sup>37</sup>  
 V. Balagura,<sup>11</sup> K. Belous,<sup>10</sup> U. Bitenc,<sup>12</sup> A. Bondar,<sup>1</sup> A. Bozek,<sup>26</sup> M. Bračko,<sup>19,12</sup> T. E. Browder,<sup>6</sup>  
 Y. Chao,<sup>25</sup> A. Chen,<sup>23</sup> W. T. Chen,<sup>23</sup> B. G. Cheon,<sup>5</sup> R. Chistov,<sup>11</sup> Y. Choi,<sup>36</sup> J. Dalseno,<sup>20</sup> M. Dash,<sup>44</sup>  
 A. Drutskoy,<sup>3</sup> S. Eidelman,<sup>1</sup> N. Gabyshev,<sup>1</sup> B. Golob,<sup>18,12</sup> K. Hayasaka,<sup>21</sup> M. Hazumi,<sup>7</sup> D. Heffernan,<sup>31</sup>  
 Y. Hoshi,<sup>39</sup> W.-S. Hou,<sup>25</sup> H. J. Hyun,<sup>16</sup> T. Iijima,<sup>21</sup> K. Inami,<sup>21</sup> A. Ishikawa,<sup>33</sup> H. Ishino,<sup>41</sup> M. Iwasaki,<sup>40</sup>  
 Y. Iwasaki,<sup>7</sup> J. H. Kang,<sup>45</sup> N. Katayama,<sup>7</sup> H. Kawai,<sup>2</sup> H. J. Kim,<sup>16</sup> S. K. Kim,<sup>35</sup> Y. J. Kim,<sup>4</sup> P. Križan,<sup>18,12</sup>  
 P. Krokovny,<sup>7</sup> R. Kumar,<sup>32</sup> C. C. Kuo,<sup>23</sup> Y.-J. Kwon,<sup>45</sup> J. Lee,<sup>35</sup> S. E. Lee,<sup>35</sup> T. Lesiak,<sup>26</sup> S.-W. Lin,<sup>25</sup> Y. Liu,<sup>4</sup>  
 D. Liventsev,<sup>11</sup> F. Mandl,<sup>9</sup> S. McOnie,<sup>37</sup> T. Medvedeva,<sup>11</sup> W. Mitaroff,<sup>9</sup> K. Miyabayashi,<sup>22</sup> H. Miyake,<sup>31</sup>  
 H. Miyata,<sup>28</sup> G. R. Moloney,<sup>20</sup> M. Nakao,<sup>7</sup> Z. Natkaniec,<sup>26</sup> S. Nishida,<sup>7</sup> O. Nitoh,<sup>43</sup> T. Ohshima,<sup>21</sup>  
 S. Okuno,<sup>13</sup> S. L. Olsen,<sup>6,8</sup> W. Ostrowicz,<sup>26</sup> H. Ozaki,<sup>7</sup> P. Pakhlov,<sup>11</sup> G. Pakhlova,<sup>11</sup> H. Park,<sup>16</sup> K. S. Park,<sup>36</sup>  
 R. Pestotnik,<sup>12</sup> L. E. Piilonen,<sup>44</sup> N. Sasao,<sup>15</sup> O. Schneider,<sup>17</sup> K. Senyo,<sup>21</sup> M. E. Sevier,<sup>20</sup> M. Shapkin,<sup>10</sup>  
 H. Shibuya,<sup>38</sup> J.-G. Shiu,<sup>25</sup> A. Somov,<sup>3</sup> S. Stanič,<sup>29</sup> M. Starič,<sup>12</sup> K. Sumisawa,<sup>7</sup> T. Sumiyoshi,<sup>42</sup> F. Takasaki,<sup>7</sup>  
 K. Tamai,<sup>7</sup> N. Tamura,<sup>28</sup> M. Tanaka,<sup>7</sup> Y. Teramoto,<sup>30</sup> T. Tsuboyama,<sup>7</sup> S. Uehara,<sup>7</sup> T. Uglov,<sup>11</sup> Y. Unno,<sup>5</sup>  
 S. Uno,<sup>7</sup> P. Urquijo,<sup>20</sup> G. Varner,<sup>6</sup> K. E. Varvell,<sup>37</sup> K. Vervink,<sup>17</sup> S. Villa,<sup>17</sup> C. C. Wang,<sup>25</sup> C. H. Wang,<sup>24</sup>  
 M.-Z. Wang,<sup>25</sup> P. Wang,<sup>8</sup> M. Watanabe,<sup>28</sup> Y. Watanabe,<sup>13</sup> J. Wicht,<sup>17</sup> E. Won,<sup>14</sup> Y. Yamashita,<sup>27</sup>  
 M. Yamauchi,<sup>7</sup> C. Z. Yuan,<sup>8</sup> Y. Yusa,<sup>44</sup> C. C. Zhang,<sup>8</sup> Z. P. Zhang,<sup>34</sup> V. Zhilich,<sup>1</sup> and A. Zupanc<sup>12</sup>

(The Belle Collaboration)

<sup>1</sup>*Budker Institute of Nuclear Physics, Novosibirsk*

<sup>2</sup>*Chiba University, Chiba*

<sup>3</sup>*University of Cincinnati, Cincinnati, Ohio 45221*

<sup>4</sup>*The Graduate University for Advanced Studies, Hayama*

<sup>5</sup>*Hanyang University, Seoul*

<sup>6</sup>*University of Hawaii, Honolulu, Hawaii 96822*

<sup>7</sup>*High Energy Accelerator Research Organization (KEK), Tsukuba*

<sup>8</sup>*Institute of High Energy Physics, Chinese Academy of Sciences, Beijing*

<sup>9</sup>*Institute of High Energy Physics, Vienna*

<sup>10</sup>*Institute of High Energy Physics, Protvino*

<sup>11</sup>*Institute for Theoretical and Experimental Physics, Moscow*

<sup>12</sup>*J. Stefan Institute, Ljubljana*

<sup>13</sup>*Kanagawa University, Yokohama*

<sup>14</sup>*Korea University, Seoul*

<sup>15</sup>*Kyoto University, Kyoto*

<sup>16</sup>*Kyungpook National University, Taegu*

<sup>17</sup>*École Polytechnique Fédérale de Lausanne (EPFL), Lausanne*

<sup>18</sup>*University of Ljubljana, Ljubljana*

<sup>19</sup>*University of Maribor, Maribor*

<sup>20</sup>*University of Melbourne, School of Physics, Victoria 3010*

<sup>21</sup>*Nagoya University, Nagoya*

<sup>22</sup>*Nara Women's University, Nara*

<sup>23</sup>*National Central University, Chung-li*

<sup>24</sup>*National United University, Miao Li*

<sup>25</sup>*Department of Physics, National Taiwan University, Taipei*

<sup>26</sup>*H. Niewodniczanski Institute of Nuclear Physics, Krakow*

<sup>27</sup>*Nippon Dental University, Niigata*

<sup>28</sup>*Niigata University, Niigata*

<sup>29</sup>*University of Nova Gorica, Nova Gorica*

<sup>30</sup>*Osaka City University, Osaka*

<sup>31</sup>*Osaka University, Osaka*

<sup>32</sup>*Panjab University, Chandigarh*

<sup>33</sup>*Saga University, Saga*

<sup>34</sup>*University of Science and Technology of China, Hefei*

<sup>35</sup>*Seoul National University, Seoul*

<sup>36</sup>*Sungkyunkwan University, Suwon*

<sup>37</sup>*University of Sydney, Sydney, New South Wales*

<sup>38</sup>Toho University, Funabashi<sup>39</sup>Tohoku Gakuin University, Tagajo<sup>40</sup>Department of Physics, University of Tokyo, Tokyo<sup>41</sup>Tokyo Institute of Technology, Tokyo<sup>42</sup>Tokyo Metropolitan University, Tokyo<sup>43</sup>Tokyo University of Agriculture and Technology, Tokyo<sup>44</sup>Virginia Polytechnic Institute and State University, Blacksburg, Virginia 24061<sup>45</sup>Yonsei University, Seoul

We report an observation of the decay  $B^\pm \rightarrow \phi\phi K^\pm$  and evidence for  $B^0 \rightarrow \phi\phi K^0$ . These results are based on a  $414 \text{ fb}^{-1}$  data sample collected with the Belle detector at the KEKB asymmetric-energy  $e^+e^-$  collider operating at the  $\Upsilon(4S)$  resonance. The branching fractions for these decay modes are measured to be  $\mathcal{B}(B^\pm \rightarrow \phi\phi K^\pm) = (3.2_{-0.5}^{+0.6} \pm 0.3) \times 10^{-6}$  and  $\mathcal{B}(B^0 \rightarrow \phi\phi K^0) = (2.3_{-0.7}^{+1.0} \pm 0.2) \times 10^{-6}$  for  $\phi\phi$  invariant mass below  $2.85 \text{ GeV}/c^2$ . The corresponding partial rate asymmetry for the charged  $B$  mode is measured to be  $\mathcal{A}_{CP}(B^\pm \rightarrow \phi\phi K^\pm) = 0.01_{-0.16}^{+0.19} \pm 0.02$ . We also study the decays  $B^\pm \rightarrow J/\psi K^\pm$  and  $B^\pm \rightarrow \eta_c K^\pm$ , where the  $J/\psi$  and  $\eta_c$  decay to final states with four charged kaons. We find  $\mathcal{A}_{CP}(B^\pm \rightarrow \phi\phi K^\pm)$  with the  $\phi\phi$  candidates within the  $\eta_c$  mass region is  $0.15_{-0.17}^{+0.16} \pm 0.02$ , consistent with no asymmetry.

PACS numbers: 13.25.Ft, 13.25.Hw, 14.40.Nd

Evidence of charmless  $B \rightarrow \phi\phi K$  decays has been reported by the Belle collaboration using  $85 \times 10^6 B\bar{B}$  pairs [1]. In the Standard Model (SM), this decay channel requires the creation of an additional final  $s\bar{s}$  quark pair in a  $b \rightarrow s\bar{s}$  process, such as  $B \rightarrow \phi K$ . Therefore, the study of  $B \rightarrow \phi\phi K$  provides useful information for understanding quark fragmentation in  $B$  decays. Moreover, our previous study also reported results for the decays  $B \rightarrow J/\psi K(\eta_c K)$  with the  $J/\psi(\eta_c)$  decaying into four kaons in the final state, which can proceed with  $\phi$  mesons in the intermediate state. It has been suggested that large direct  $CP$  violation up to 40% is possible in  $B \rightarrow \eta_c K \rightarrow \phi\phi K$  if there is a sizable  $b \rightarrow s$  transition with a non-SM  $CP$ -violating phase that interferes with the decay amplitude via the  $\eta_c$  resonance [2].

Recently the BaBar collaboration has reported results of a study of  $B \rightarrow \phi\phi K$  [3]. The branching fraction for  $B^\pm \rightarrow \phi\phi K^\pm$  that they obtained is around three times larger than our previous measurement [1]. Here we present improved measurements of  $B \rightarrow \phi\phi K$  decays with not only larger statistics but also proper consideration of the non-resonant  $K^+K^-$  contribution underneath the  $\phi$  resonance. The analysis is based on a data sample of  $414 \text{ fb}^{-1}$  containing  $449 \times 10^6 B\bar{B}$  pairs. The data were collected with the Belle detector at the KEKB asymmetric-energy  $e^+e^-$  (3.5 on 8 GeV) collider [4] operating at the  $\Upsilon(4S)$  resonance.

The Belle detector is a large-solid-angle magnetic spectrometer that consists of a silicon vertex detector (SVD), a 50-layer central drift chamber (CDC), an array of aerogel threshold Cherenkov counters (ACC), a barrel-like arrangement of time-of-flight scintillation counters (TOF), and an electromagnetic calorimeter comprised of CsI(Tl) crystals (ECL) located inside a superconducting solenoid coil that provides a 1.5 T magnetic field. An iron flux-return located outside the coil is instrumented to detect

$K_L^0$  mesons and to identify muons (KLM). The detector is described in detail elsewhere [5]. Two inner detector configurations were used. A 2.0 cm radius beampipe and a 3-layer silicon vertex detector (SVD1) were used for the first sample of  $152 \times 10^6 B\bar{B}$  pairs, while a 1.5 cm radius beampipe, a 4-layer silicon detector (SVD2) and a small-cell inner drift chamber were used to record the remaining  $297 \times 10^6 B\bar{B}$  pairs [6].

Charged kaons are required to have impact parameters within  $\pm 2 \text{ cm}$  of the interaction point (IP) along the  $z$ -axis (antiparallel to the positron direction) and within 0.2 cm in the transverse plane. Each track is identified as a kaon or a pion according to a  $K/\pi$  likelihood ratio,  $\mathcal{R}(K/\pi) = \mathcal{L}_K/(\mathcal{L}_K + \mathcal{L}_\pi)$ , where  $\mathcal{L}_K/\mathcal{L}_\pi$  is the likelihood of kaons/pions derived from the responses of TOF and ACC systems and the energy loss measurements from the CDC. The likelihood ratio is required to exceed 0.6 for kaon candidates; within the momentum range of interest, this requirement is 88% efficient for kaons and has a misidentification rate for pions of 8.5%. Neutral kaons are reconstructed via the decay  $K_S^0 \rightarrow \pi^+\pi^-$  and have an invariant mass  $0.482 \text{ GeV}/c^2 < M_{\pi^+\pi^-} < 0.514 \text{ GeV}/c^2$  ( $\pm 4\sigma$  mass resolution). The  $\pi^+\pi^-$  vertex is required to be displaced from the IP and the flight direction must be consistent with a  $K_S^0$  that originated from the IP. The required displacement increases with the momentum of the  $K_S^0$  candidate.

$B$  meson candidates are reconstructed in the five-kaon final state. Two kinematic variables are used to distinguish signal candidates from backgrounds: the beam-energy constrained mass  $M_{bc} = \sqrt{E_{\text{beam}}^2 - |\vec{P}_{\text{recon}}|^2}$  and the energy difference  $\Delta E = E_{\text{recon}} - E_{\text{beam}}$ , where  $E_{\text{beam}}$  is the beam energy, and  $E_{\text{recon}}$  and  $\vec{P}_{\text{recon}}$  are the reconstructed energy and momentum of the signal candidate in the  $\Upsilon(4S)$  rest frame. The resolution of  $M_{bc}$  is approximately  $2.8 \text{ MeV}/c^2$ , dominated by the beam en-

ergy spread, while the  $\Delta E$  resolution is around 10 MeV. Candidates with five kaons within the region  $|\Delta E| < 0.2$  GeV and  $5.2 \text{ GeV}/c^2 < M_{bc}$  are selected for further consideration. The signal region is defined as  $5.27 \text{ GeV}/c^2 < M_{bc} < 5.29 \text{ GeV}/c^2$  and  $|\Delta E| < 0.05$  GeV.

The dominant backgrounds are  $e^+e^- \rightarrow q\bar{q}$  ( $q = u, d, s, c$ ) continuum events. Event topology and  $B$  flavor tagging are used to distinguish the jet-like continuum events and the spherically distributed  $B\bar{B}$  events. Seven event-shape variables are combined into a single Fisher discriminant [7]. The Fisher variables include the angle between the thrust axis of the  $B$  candidate and the thrust axis of the rest of the event ( $\cos\theta_T$ ), five modified Fox-Wolfram moments [8], and a measure of the momentum transverse to the event thrust axis ( $S_\perp$ ) [9]. Two other variables that are uncorrelated with the Fisher discriminant and help to distinguish signal from the continuum are  $\cos\theta_B$ , where  $\theta_B$  is the angle between the  $B$  flight direction and the beam direction in the  $e^+e^-$  center-of-mass frame, and  $\Delta z$ , the  $z$  vertex difference between the signal  $B$  candidate and its accompanying  $B$ . We form signal and background probability density functions (PDFs) for the Fisher discriminant,  $\cos\theta_B$  and  $\Delta z$  using the signal Monte Carlo (MC) events and sideband data ( $5.2 \text{ GeV}/c^2 < M_{bc} < 5.26 \text{ GeV}/c^2$ ), respectively. The products of the PDFs for these variables give signal and background likelihoods  $\mathcal{L}_S$  and  $\mathcal{L}_{BG}$  for each candidate, allowing a selection to be applied to the likelihood ratio  $\mathcal{R} = \mathcal{L}_S/(\mathcal{L}_S + \mathcal{L}_{BG})$ .

Additional background discrimination is provided by the quality of the  $B$  flavor tagging of the accompanying  $B$  meson. The standard Belle flavor tagging package [10] gives two outputs: a discrete variable indicating the flavor of the tagging  $B$  and dilution factor  $r$ , which ranges from zero for no flavor information to unity for unambiguous flavor assignment. The continuum background is reduced by applying a selection requirement on the variable  $\mathcal{R}$  for events in each  $r$  region according to the figure of merit defined as  $N_S/\sqrt{N_S + N_{BG}}$ , where  $N_S$  denotes the expected  $\phi\phi K$  signal yield based on MC simulation and the branching fraction reported in our previous measurements, and  $N_{BG}$  denotes the expected  $q\bar{q}$  yields from sideband data. This requirement removes (61-81)% of the continuum background while retaining (80-92)% of the signal, and depends on the decay channel ( $\phi\phi K$  or  $\phi\phi K^0$ ) and the SVD configuration during the measurement (SVD1 or SVD2). Backgrounds from other  $B$  decays are investigated using a large MC sample and are found to be negligible after the  $\mathcal{R}$  requirement.

The signal yields are extracted by applying an unbinned extended maximum likelihood (ML) fit to the events with  $M_{bc} > 5.2 \text{ GeV}/c^2$  and  $|\Delta E| < 0.2$  GeV. For the  $\phi\phi K^\pm$  mode, we simultaneously obtain the yield and the partial rate asymmetry  $\mathcal{A}_{CP}$  using the likelihood, defined as:

$$\mathcal{L} = e^{-(N_S + N_{BG})} \prod_i^N \left( \sum_j \frac{1}{2} [1 - q_i \cdot \mathcal{A}_{CP}^j] N_j P_i^j \right), \quad (1)$$

where  $i$  is the identifier of the  $i$ -th event,  $j$  indicates signal ( $S$ ) or background ( $BG$ ),  $P$  is the two-dimensional PDF of  $M_{bc}$  and  $\Delta E$ , and  $q$  indicates the  $B$  meson flavor, +1 for  $B^+$  and -1 for  $B^-$ , respectively. For neutral  $B$  events, the factor  $\frac{1}{2}[1 - q_i \cdot \mathcal{A}_{CP}]$  in Eq. (1) is replaced by 1. The  $M_{bc}$  PDFs are modeled by a Gaussian function for signals and an ARGUS function [11] for the continuum, while a Gaussian is used to describe the signal  $\Delta E$  and a second-order Chebyshev polynomial is used for the background  $\Delta E$  distribution. The parameters of the PDFs are determined using high-statistics MC samples and sideband data for signal and background shapes, respectively. The signal PDFs are calibrated by comparing the  $M_{bc}$  and  $\Delta E$  distributions of the  $B^+ \rightarrow \bar{D}^0(K^+\pi^-\pi^-\pi^+)\pi^+$  data with the MC expectation.

We search for charmless  $B \rightarrow \phi\phi K$  decays by requiring the  $\phi\phi$  invariant mass ( $M_{\phi\phi}$ ) to be less than  $2.85 \text{ GeV}/c^2$ , the region below charmonium threshold. Candidate  $\phi$  mesons are identified by requiring the invariant masses of  $K^+K^-$  pairs ( $M_{K^+K^-}$ ) to be in the range  $1.0 \text{ GeV}/c^2$  to  $1.04 \text{ GeV}/c^2$  ( $\pm 4.6\sigma$ ). Figure 1 shows the  $M_{bc}$  and  $\Delta E$  projections with the fit curves superimposed. Clear signals appear in both  $B^\pm$  and  $B^0$  modes with signal yields of  $37.0_{-6.0}^{+6.7}$  and  $7.8_{-2.5}^{+3.2}$ , respectively. Although  $K^+K^-$  candidates are required to lie in the  $\phi$  mass region, non- $\phi$  backgrounds may also contribute. Figure 2(a) shows the  $M_{K^+K^-}^1$  vs.  $M_{K^+K^-}^2$  distributions for  $(K^+K^-K^+K^-)K^\pm$  candidates in the signal region, where the two  $K^+K^-$  pairs are required to have invariant masses less than  $1.2 \text{ GeV}/c^2$ . Events in the two  $\phi$  bands are used to estimate the  $B^\pm \rightarrow \phi K^+K^-K^\pm$  contribution. Figure 2(b) shows the  $B$  signal yields [12] as a function of the  $K^+K^-$  invariant mass after requiring the other  $K^+K^-$  pair to have a mass in the  $\phi$  mass region. The  $B$  signal yields are fitted with a threshold function in the region  $0.98 \text{ GeV}/c^2 < M_{K^+K^-} < 1.20 \text{ GeV}/c^2$ , excluding the  $\phi$  mass region ( $1.00 \text{ GeV}/c^2 < M_{K^+K^-} < 1.04 \text{ GeV}/c^2$ ). The size of the non- $\phi$  contribution is estimated by interpolating the  $B$  yields in the  $\phi$  sideband region to the  $\phi$  mass region. Since events in the two  $\phi$  bands contain both true  $\phi$  mesons and non-resonant  $K^+K^-$  pairs, the area underneath the  $\phi$  mass region in Fig. 2(b) also includes the  $\phi K^+K^-K^\pm$  contribution and, due to combinatorics, a double counted contribution from the non-resonant  $5K$  component. The contribution of  $B \rightarrow 5K$  is estimated by extrapolating the  $B$  signal yield in the upper right corner of the dashed region in Fig. 2(a) to the  $\phi$  mass region. The fraction of non- $\phi\phi K$  events in the  $\phi$  mass region as obtained from both contributions is thus  $(7 \pm 4)\%$ . The same procedure is applied to the

$\phi\phi K^0$  sample; here we obtain a fraction of  $(7 \pm 9)\%$ .

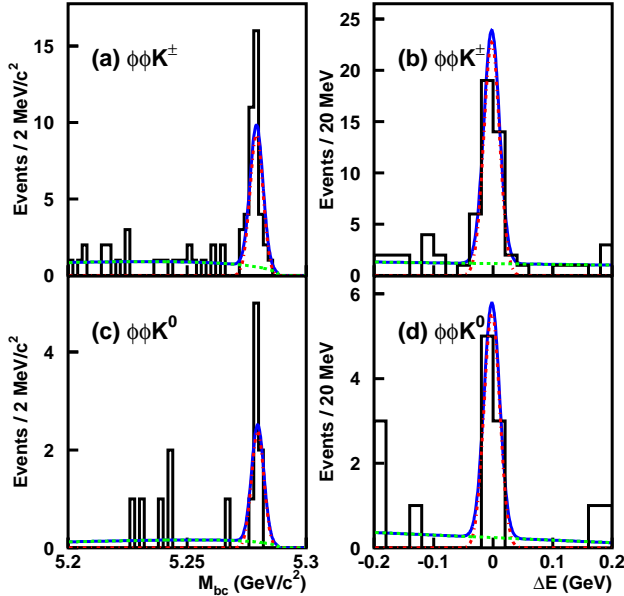


FIG. 1: Distributions of  $M_{bc}$  and  $\Delta E$  for the decay modes  $B^\pm \rightarrow \phi\phi K^\pm$  (a,b) and  $B^0 \rightarrow \phi\phi K^0$  (c,d), with  $\phi\phi$  invariant mass less than  $2.85 \text{ GeV}/c^2$ . The open histograms are the data, the solid curves show the result of the fit, the dash-dotted curves represent the signal contributions and the dashed curves show the continuum background contributions.

Table I summarizes the  $\phi\phi K$  results after subtracting the non- $\phi\phi K$  contribution. Signal efficiencies are obtained by generating  $\phi\phi K$  MC events, where the same  $M_{\phi\phi} < 2.85 \text{ GeV}/c^2$  requirement is applied. Systematic uncertainties in the fit are obtained by performing fits in which the signal peak positions and resolutions of the signal PDFs are successively varied by  $\pm 1\sigma$ . The quadratic sum of each deviation from the central value of the fit gives the systematic uncertainty of the fit. For each systematic check, the statistical significance is taken as  $\sqrt{-2 \ln(\mathcal{L}_{\text{feeddown}}/\mathcal{L}_{\text{max}})}$ , where  $\mathcal{L}_{\text{feeddown}}$  and  $\mathcal{L}_{\text{max}}$  are the likelihoods at the expected non- $\phi\phi K$  yields and the best fit, respectively. The change in significance that arises from uncertainties in the signal PDFs is negligible ( $< 1\%$ ). We choose the significance calculated after increasing the non- $\phi\phi K$  yield by its  $1\sigma$  statistical uncertainty as our significance including systematic uncertainty. The numbers of  $B^+ B^-$  and  $B^0 \bar{B}^0$  pairs are assumed to be equal.

The systematic uncertainty resulting from the  $\mathcal{R}$  requirement is studied by checking the data-MC efficiency ratio using the  $B^+ \rightarrow \bar{D}^0 (\rightarrow K^+ \pi^- \pi^- \pi^+) \pi^+$  sample. The corresponding systematic error is 2.7-2.8% and again depends on the decay channel and SVD geometry. The systematic errors on the charged track reconstruction are

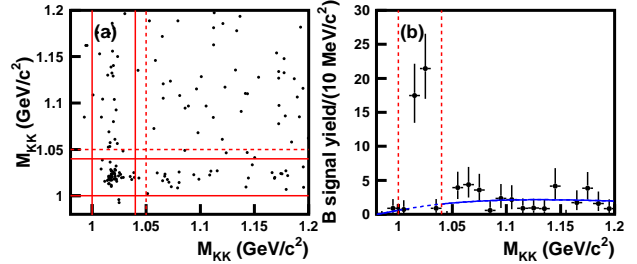


FIG. 2: (a) The distribution of  $M_{K^+K^-}^1$  vs.  $M_{K^+K^-}^2$  for the  $K^+ K^- K^+ K^- K^\pm$  candidates in the  $M_{bc} - \Delta E$  signal box with  $M_{K^+K^-} < 1.2 \text{ GeV}/c^2$ . The two  $K^+ K^-$  bands indicate the  $\phi$  mass region ( $1.0 \text{ GeV}/c^2 < M_{K^+K^-} < 1.04 \text{ GeV}/c^2$ ). The horizontal and vertical dashed lines are located at  $M_{K^+K^-} = 1.05 \text{ GeV}/c^2$ . The rectangle on the upper right is the  $\phi\phi$  sideband region; events in this region are used to estimate the non-resonant  $B \rightarrow 5K$  contribution. (b)  $B$  signal yield as a function of the  $M_{K^+K^-}$  after requiring the other  $K^+ K^-$  pair to have a mass in the  $\phi$  mass region. A threshold function is used to fit the data; events with  $1.0 \text{ GeV}/c^2 < M_{K^+K^-} < 1.04 \text{ GeV}/c^2$  are excluded when the fit is performed.

estimated to be around 1% per track using partially reconstructed  $D^*$  events. Therefore, the tracking systematic error is 5% (five tracks) for the  $\phi\phi K^\pm$  mode and 4% for the  $\phi\phi K^0$  mode (excluding  $K_S^0$  reconstruction). The kaon identification efficiency is studied using samples of inclusive  $D^{*+} \rightarrow D^0 \pi^+$ ,  $D^0 \rightarrow K^- \pi^+$  decays. The  $K_S^0$  reconstruction is verified by comparing the ratio of  $D^+ \rightarrow K_S^0 \pi^+$  and  $D^+ \rightarrow K^- \pi^+ \pi^+$  yields. The resulting  $K_S^0$  detection systematic error is 4.9%. The uncertainty in the number of  $B\bar{B}$  events is 1.4%. The final systematic error is obtained by summing all correlated errors linearly and then quadratically summing the uncorrelated errors.

After subtracting the non- $\phi\phi K$  contribution, the branching fractions for charmless  $B \rightarrow \phi\phi K$  decays are  $\mathcal{B}(B^\pm \rightarrow \phi\phi K^\pm) = (3.2_{-0.5}^{+0.6} \pm 0.3) \times 10^{-6}$  with a  $9.5\sigma$  significance and  $\mathcal{B}(B^0 \rightarrow \phi\phi K^0) = (2.3_{-0.7}^{+1.0} \pm 0.2) \times 10^{-6}$  with a  $4.7\sigma$  significance. The measured charge asymmetry for  $B^\pm \rightarrow \phi\phi K^\pm$  decay is  $0.01_{-0.16}^{+0.19} \pm 0.02$ . The first error is statistical and the second is systematic.

It is of interest to search for possible  $\phi\phi$  resonances above charmonium threshold. Figure 3(a) shows the  $B$  signal yield divided by the bin size as a function of  $M_{\phi\phi}$  if the  $M_{\phi\phi} < 2.85 \text{ GeV}/c^2$  requirement is not applied. There is no enhancement in the high  $\phi\phi$  mass region except for the  $\eta_c$  peak near  $3 \text{ GeV}/c^2$ . Reference [2] suggests the possibility of a large  $CP$  asymmetry, which could arise from the interference between  $B^\pm \rightarrow \phi\phi K^\pm$  and  $B^\pm \rightarrow \eta_c (\rightarrow \phi\phi) K^\pm$  decays. Events with  $\phi\phi$  invariant mass within  $\pm 40 \text{ MeV}/c^2$  of the nominal  $\eta_c$  mass are selected to investigate this asymmetry. The measured  $CP$  asymmetry is  $0.15_{-0.17}^{+0.16} \pm 0.02$ , which is consistent

TABLE I: Mode, yield, efficiency including secondary branching fractions, branching fraction for  $B \rightarrow \phi\phi K$  and related charmonium decays.

Mode	Yield	Efficiency(%)	$\mathcal{B}(10^{-6})$
$B^\pm \rightarrow \phi\phi K^\pm$ ( $M_{\phi\phi} < 2.85 \text{ GeV}/c^2$ )	$34.2^{+6.4}_{-5.8}$	2.41	$3.2^{+0.6}_{-0.5} \pm 0.3$
$B^0 \rightarrow \phi\phi K^0$ ( $M_{\phi\phi} < 2.85 \text{ GeV}/c^2$ )	$7.3^{+3.0}_{-2.4}$	0.69	$2.3^{+1.0}_{-0.7} \pm 0.2$
$B^\pm \rightarrow \eta_c K^\pm, \eta_c \rightarrow \phi\phi$	$27.9^{+7.3}_{-6.9}$	2.72	$2.3 \pm 0.6 \pm 0.2$
$B^\pm \rightarrow \eta_c K^\pm, \eta_c \rightarrow \phi K^+ K^-$	$60.3^{+12.2}_{-11.8}$	4.85	$2.8^{+0.6}_{-0.5} \pm 0.2$
$B^\pm \rightarrow \eta_c K^\pm, \eta_c \rightarrow 2(K^+ K^-)$	$105.7^{+26.1}_{-20.7}$	9.93	$2.4^{+0.6}_{-0.5} \pm 0.2$
$B^\pm \rightarrow J/\psi K^\pm, J/\psi \rightarrow \phi K^+ K^-$	$26.3^{+6.9}_{-6.1}$	4.67	$1.3 \pm 0.3 \pm 0.2$
$B^\pm \rightarrow J/\psi K^\pm, J/\psi \rightarrow 2(K^+ K^-)$	$36.0^{+7.7}_{-7.3}$	9.41	$0.85^{+0.18}_{-0.17} \pm 0.10$

with no asymmetry.

We study possible charmonium states by measuring the  $B$  yield with  $M_{4K}$  between  $2.8 \text{ GeV}/c^2$  and  $3.2 \text{ GeV}/c^2$ . Since  $\eta_c$  and  $J/\psi$  mesons may decay to  $\phi K^+ K^-$  and  $2(K^+ K^-)$ , mass fits are performed with and without the requirement that one or both  $K^+ K^-$  pairs lie in the  $\phi$  mass region. As shown in Fig. 3, clear  $\eta_c$  and  $J/\psi$  resonances are visible in the  $\phi K^+ K^-$  and  $4K$  samples while only an  $\eta_c$  peak appears in the  $\phi\phi$  mode.

We obtain the signal yields for  $B^\pm \rightarrow \eta_c K^\pm$  and  $B^\pm \rightarrow J/\psi K^\pm$  by performing  $\chi^2$  fits with asymmetric errors to the  $M_{\phi\phi}$ ,  $M_{\phi K^+ K^-}$  and  $M_{4K}$  invariant mass distributions, which are presented in Figs. 3(b, c, d). The  $J/\psi$  signal PDF is modeled with a Gaussian function while the  $\eta_c$  PDF is described by a Breit-Wigner function convoluted with a Gaussian resolution function, which has the same Gaussian width as the  $J/\psi$  PDF. Since sizable signals are observed in the  $4K$  mode, the parameters are determined using the  $4K$  sample and the same signal PDFs are then applied to the  $\phi K^+ K^-$  and  $\phi\phi$  samples. The obtained Gaussian width is measured to be  $4.5^{+1.9}_{-1.3} \text{ MeV}/c^2$ . The resulting signal yields are summarized in Table I. The peak positions obtained for the  $\eta_c$  and  $J/\psi$  are  $2.979 \pm 0.002 \pm 0.001 \text{ GeV}/c^2$  and  $3.094 \pm 0.001 \text{ GeV}/c^2$ , respectively, consistent with the nominal  $\eta_c$  and  $J/\psi$  masses. The  $\eta_c$  Breit-Wigner width is measured to be  $29.8^{+12.2}_{-8.5} \pm 0.1 \text{ MeV}/c^2$ , where the central value is consistent with the world average [13] and the second error is due to the uncertainty of the Gaussian width for the mass resolution. The validity of determining  $B$  signal yields from a constrained  $\chi^2$  fit with an asymmetric error is verified by toy MC.

For the  $\phi K^+ K^-$  and  $\phi\phi$  modes, the non- $\phi$  contribution is determined from the  $B$  signal yields for events with one  $K^+ K^-$  pair in the  $\phi$  sideband region ( $1.05 \text{ GeV}/c^2 < M_{K^+ K^-} < 1.09 \text{ GeV}/c^2$ ) and the  $4K$  and  $\phi K^+ K^-$  masses in the charmonium resonance region, respectively. We find  $3.0^{+2.1}_{-1.4}$  events in the  $\eta_c \rightarrow \phi\phi$  mode,  $6.4^{+5.4}_{-4.5}$  events in the  $\eta_c \rightarrow \phi K^+ K^-$  mode, and  $3.5^{+3.6}_{-2.6}$  events in the  $J/\psi \rightarrow \phi K^+ K^-$  mode. For the yields of these modes, listed in Table I, the corresponding feed-down yields have been subtracted.

Signal efficiencies are determined using signal MC and

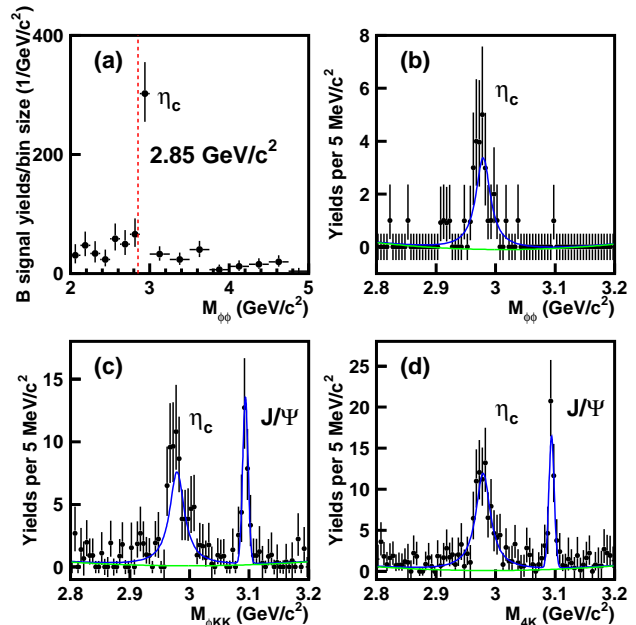


FIG. 3:  $B^\pm$  signal yield as a function of (a,b)  $M_{\phi\phi}$ , (c)  $M_{\phi K^+ K^-}$  and (d)  $M_{4K}$ . In (a) we use different bin sizes for  $M_{\phi\phi}$  less than  $3 \text{ GeV}/c^2$  and greater than  $3 \text{ GeV}/c^2$ . The subset with  $M_{\phi\phi}$  from  $2.8 \text{ GeV}/c^2$  to  $3.2 \text{ GeV}/c^2$  is shown in (b). The  $J/\psi$  signal PDF is modeled with a Gaussian function while the  $\eta_c$  PDF is described by a Breit-Wigner function convoluted with a Gaussian resolution function, which has the same Gaussian width as the  $J/\psi$  PDF. The solid curves in (b,c,d) show the results of the fit and the contributions (second order polynomial) not from the  $J/\psi$  and  $\eta_c$ .

their systematic uncertainties are similar to what was described in the charmless  $\phi\phi K$  part. Systematic uncertainties in the fitting are obtained by performing fits in which the signal peak positions, the resolutions of the signal PDF's and the width of the Gaussian resolution function convoluted with the  $\eta_c$  PDF are successively varied by  $\pm\sigma$ . The quadratic sum of all deviations gives the systematic error of the fit. The products of the branching fractions for various decays are listed in Table I. Since the probabilities of  $\eta_c$  and  $J/\psi$  decays to  $4K$ ,  $\phi K K$  and

$\phi\phi$  final states are measured with poor accuracy, we can use the values from Table I as well as the world average branching fractions  $\mathcal{B}(B^\pm \rightarrow \eta_c K^\pm) = (9.1 \pm 1.3) \times 10^{-4}$  and  $\mathcal{B}(B^\pm \rightarrow J/\psi K^\pm) = (1.007 \pm 0.035) \times 10^{-3}$  [13] to determine independently the corresponding branching fractions for the  $\eta_c$  and  $J/\psi$ ; the results are shown in Table II. The world average values given above are based on datasets, which also include Belle measurements [14]; however, our estimate shows that effects of possible correlations are negligible. We also provide the ratios of branching fractions as shown in Table III. The systematic uncertainties are predominately due to the Gaussian width for the mass resolution; other systematic uncertainties either cancel out in the ratios or too small to be considered.

TABLE II: The measured branching fractions of secondary charmonium decays.

Decay mode	$\mathcal{B}$
$\eta_c \rightarrow \phi\phi$	$(2.5^{+0.7}_{-0.6} \pm 0.4) \times 10^{-3}$
$\eta_c \rightarrow \phi K^+ K^-$	$(3.0 \pm 0.6 \pm 0.5) \times 10^{-3}$
$\eta_c \rightarrow 2(K^+ K^-)$	$(2.6^{+0.6}_{-0.5} \pm 0.4) \times 10^{-3}$
$J/\psi \rightarrow \phi K^+ K^-$	$(1.2 \pm 0.3 \pm 0.2) \times 10^{-3}$
$J/\psi \rightarrow 2(K^+ K^-)$	$(8.5^{+1.8}_{-1.7} \pm 1.0) \times 10^{-4}$

TABLE III: Ratios of branching fractions for the  $\eta_c$  and  $J/\psi$  decays.

Mode	Ratio
$\frac{\mathcal{B}(\eta_c \rightarrow \phi\phi)}{\mathcal{B}(\eta_c \rightarrow 2(K^+ K^-))}$	$0.96^{+0.20}_{-0.24} \pm 0.02$
$\frac{\mathcal{B}(\eta_c \rightarrow \phi K^+ K^-)}{\mathcal{B}(\eta_c \rightarrow 2(K^+ K^-))}$	$1.17^{+0.33}_{-0.36} \pm 0.01$
$\frac{\mathcal{B}(J/\psi \rightarrow \phi K^+ K^-)}{\mathcal{B}(J/\psi \rightarrow 2(K^+ K^-))}$	$1.47^{+0.49+0.06}_{-0.46-0.08}$

In summary, we have observed the charmless decay  $B^\pm \rightarrow \phi\phi K^\pm$  and evidence for  $B^0 \rightarrow \phi\phi K^0$ . We also report the  $CP$  asymmetry of the charged decay and measurements of other closely related charmonium decays. The results are consistent with our previous measurements [1] and supersede them, and have considerably better precision due to the increase in statistics. The obtained branching fraction of charmless  $B^\pm \rightarrow \phi\phi K^\pm$  decay is  $3.1\sigma$  smaller than the measurement by the BaBar collaboration [3]. For the charmonium decays, we find that the decay  $\eta_c \rightarrow \phi\phi$  contributes around 42% and 24% of the  $\eta_c \rightarrow \phi K^+ K^-$  and  $\eta_c \rightarrow 2(K^+ K^-)$  events, respectively. The latter is consistent with an early Belle measurement [15] using  $\eta_c$  events produced in two pho-

ton collisions. For both the  $\eta_c$  and  $J/\psi$  decays into four charged kaons, the  $\phi K^+ K^-$  contribution dominates.

We thank the KEKB group for excellent operation of the accelerator, the KEK cryogenics group for efficient solenoid operations, and the KEK computer group and the NII for valuable computing and Super-SINET network support. We acknowledge support from MEXT and JSPS (Japan); ARC and DEST (Australia); NSFC and KIP of CAS (China); DST (India); MOEHRD, KOSEF and KRF (Korea); KBN (Poland); MES and RFAAE (Russia); ARRS (Slovenia); SNSF (Switzerland); NSC and MOE (Taiwan); and DOE (USA).

- 
- [1] H.C. Huang *et al.* (Belle Collaboration), Phys. Rev. Lett. **91**, 241802 (2003).
  - [2] M. Hazumi, Phys. Lett. B **583**, 285 (2004).
  - [3] B. Aubert *et al.* (BABAR Collaboration), Phys. Rev. Lett. **97**, 261803 (2006).
  - [4] S. Kurokawa and E. Kikutani, Nucl. Instr. and Meth. A **499**, 1 (2003), and other papers included in this volume.
  - [5] A. Abashian *et al.* (Belle Collaboration), Nucl. Instr. and Meth. A **479**, 117 (2002).
  - [6] Y. Ushiroda, Nucl. Instr. and Meth. A **511** 6 (2003); Z. Natananec *et al.*, (Belle SVD2 Group), Nucl. Instr. and Meth. A **560**, 1 (2006).
  - [7] R. A. Fisher, Ann. Eugenics **7**, 179 (1936).
  - [8] The Fox-Wolfram moments were introduced in G. C. Fox and S. Wolfram, Phys. Rev. Lett. **41**, 1581 (1978). The Fisher discriminant used by Belle, based on modified Fox-Wolfram moments (SFW), is described in K. Abe *et al.* (Belle Collaboration), Phys. Rev. Lett. **87**, 101801 (2001) and K. Abe *et al.* (Belle Collaboration.), Phys. Lett. B **511**, 151 (2001).
  - [9] R. Ammar *et al.* (CLEO Collaboration), Phys. Rev. Lett. **71**, 674 (1993).
  - [10] H. Kakuno *et al.*, Nucl. Instr. and Meth. A **533**, 516 (2004).
  - [11] H. Albrecht *et al.* (ARGUS Collaboration), Phys. Lett. B **229**, 304 (1989).
  - [12] Hereafter in this paper, the  $B$  signal yield is obtained from 2D  $M_{bc} - \Delta E$  fits to the events in each bin of the plot.
  - [13] W.-M. Yao *et al.* (Particle Data Group), Journal of Physics G **33**, 1 (2006) and 2007 partial update for edition 2008.
  - [14] F. Fang *et al.* (Belle Collaboration), Phys. Rev. Lett. **90**, 071801 (2003); K. Abe *et al.* (Belle Collaboration), Phys. Rev. D **67**, 032003 (2003).
  - [15] S. Uehara *et al.* (Belle Collaboration), Euro. Phys. Jour. C **53**, 1 (2008).